Electron-matter interactions: Elastic scattering (III)

Duncan Alexander
EPFL-IPHYS-LSME

Contents

Part A: dynamical theory – Bloch wave approach

- 2-beam Bloch wave intensities
- Extension of Bloch wave approach to many beams
- CBED patterns; dynamical fringes and polarity effects
- Electron channeling and the *s*-state

Part B: phonon scattering

- Observations:
  - diffuse scattering in diffraction, HAADF STEM imaging, Debye-Waller factor
- Phenomenological adaptation of Bloch wave theory
- HAADF STEM imaging; Mott scattering and frozen phonon model
- Quantum mechanical model of phonon scattering

Recap: 2-beam diffracted beam intensities

- From eqs 2.17 and 2.1 total wave function is:

$$\Psi(\vec{\boldsymbol{r}}) = \sum_j \alpha^{(j)} \psi^{(j)}(\vec{\boldsymbol{r}}) = \sum_j \alpha^{(j)} \sum_g C_g^{(j)} \exp\left[2\pi i\left(\vec{\boldsymbol{k}}^{(j)} + \vec{\boldsymbol{g}}\right)\cdot \vec{\boldsymbol{r}}\right] \tag{2.33}$$

- 2-beam approximation:

$$C_0^{(1)} = C_0^{(2)} = C_g^{(1)} = -C_g^{(2)} = \frac{1}{\sqrt{2}} \tag{2.37}$$

$$I_g(t) = \frac{1}{1+\xi_g^2 s^2}\sin^2\left(\pi t\sqrt{\frac{1}{\xi_g^2}+s^2}\right) \qquad I_0(t) = 1 - I_g(t) \tag{2.40}$$

Wave function intensities *at exact Bragg*

- Going back to wave function, from eqs 2.33 and 2.37 for exact Bragg can obtain:

$$\psi^{(1)}(\vec{\boldsymbol{r}}) = \cos(\pi \vec{\boldsymbol{g}} \cdot \vec{\boldsymbol{r}}) \exp\left[2\pi i\left(\vec{\boldsymbol{k}}^{(1)} + 0.5\vec{\boldsymbol{g}}\right) \cdot \vec{\boldsymbol{r}}\right] \tag{2.41}$$

$$\psi^{(2)}(\vec{\boldsymbol{r}}) = i \sin(\pi \vec{\boldsymbol{g}} \cdot \vec{\boldsymbol{r}}) \exp\left[2\pi i\left(\vec{\boldsymbol{k}}^{(2)} + 0.5\vec{\boldsymbol{g}}\right) \cdot \vec{\boldsymbol{r}}\right] \tag{2.42}$$

- Choosing coordinate x parallel to $\vec{\boldsymbol{g}}$ with origin of $\vec{\boldsymbol{r}}$ at an atomic site (also centre of symmetry), electron density in each Bloch wave is then:

$$\left|\psi^{(1)}(\vec{\boldsymbol{r}})\right|^2 = \cos^2(\pi g x) \tag{2.43}$$

$$\left|\psi^{(2)}(\vec{\boldsymbol{r}})\right|^2 = \sin^2(\pi g x) \tag{2.44}$$

Wave function intensities

- Type 1 wave channels down nuclei, Type 2 propagates between nuclei:

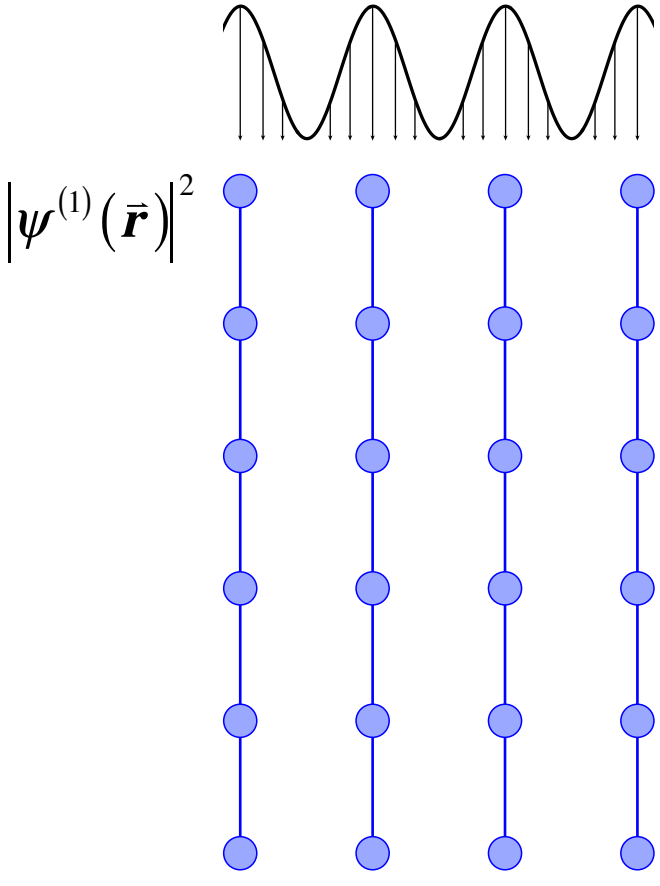

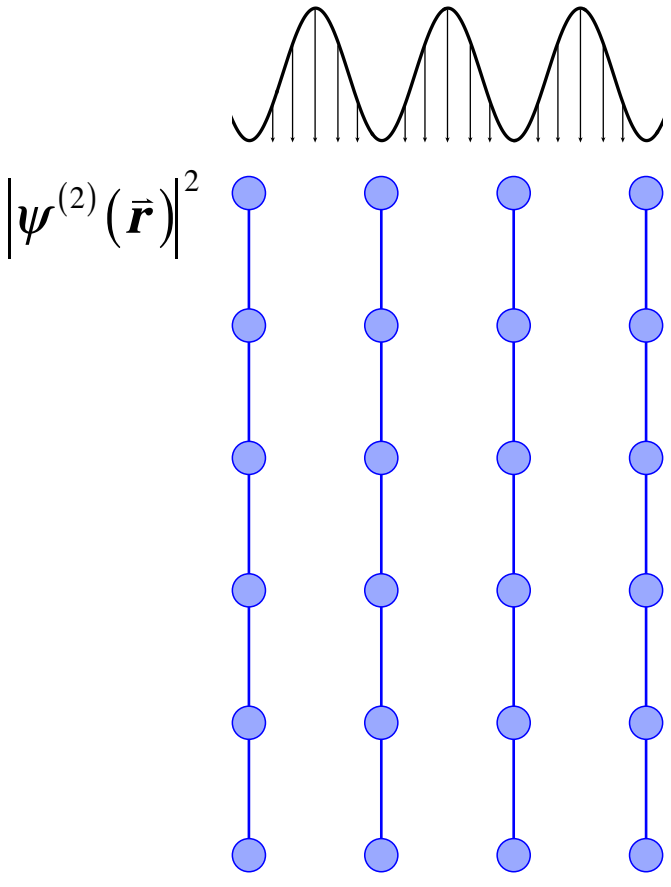

Bloch wave analysis: multiple beams

- Extend Bloch wave model to many beams
- Start from eq. 2.33: $\Psi(\vec{r}) = \sum_j \alpha^{(j)} \psi^{(j)}(\vec{r}) = \sum_j \alpha^{(j)} \sum_g C_g^{(j)} \exp\left[2\pi i\left(\vec{k}^{(j)} + \vec{g}\right)\cdot \vec{r}\right]$

- Many-beam theory eigenvalue equation (*secular* equation) is extension of 2-beam eq. 2.32:

$$\frac{1}{2\kappa}\begin{pmatrix} -k_t^2 & U_{-g} & U_{-h} & \cdots \\ U_g & -(k_t+g)^2 & U_{g-h} & \cdots \\ U_h & U_{h-g} & -(k_t+h)^2 & \cdots \\ \cdots & \cdots & \cdots & \cdots \end{pmatrix}\begin{pmatrix} C_0^{(j)} \\ C_g^{(j)} \\ C_h^{(j)} \\ \cdots \end{pmatrix} = \left(k_z^{(j)} - \kappa\right)\begin{pmatrix} C_0^{(j)} \\ C_g^{(j)} \\ C_h^{(j)} \\ \cdots \end{pmatrix} \qquad (3.1)$$

Bloch wave analysis: multiple beams

- Eq. 3.1 is of the form: $$\boldsymbol{A}\boldsymbol{C}^{(j)} = \left(k_z^{(j)} - \boldsymbol{\kappa}\right)\boldsymbol{C}^{(j)} \tag{3.2}$$
- If n beams considered (including direct beam $\vec{\boldsymbol{g}} = 0$) $\boldsymbol{A}$ is an $(n \times n)$ matrix
- There are n eigenvalues and n Bloch waves, each Bloch wave having n plane wave components
- $\boldsymbol{A}$ is Hermitian, since $U_g = U_{-g}^*$
- Eigenvalues are real and an $(n \times n)$ eigenvector matrix $\boldsymbol{C}$ matrix consisting of columns of complex eigenvectors $\boldsymbol{C}^{(j)}$ is unitary:

$$\boldsymbol{C}^{-1} = \boldsymbol{C}^{\dagger} = \tilde{\boldsymbol{C}}^{*} \tag{3.3}$$

Bloch wave analysis: multiple beams

- Written explicitly that is: $$\sum_g C_g^{(i)} C_g^{(j)*} = \delta_{ij} \quad (3.4)$$

  and: $$\sum_j C_g^{(j)} C_h^{(j)*} = \delta_{gh} \quad (3.5)$$

- Hence eigenvectors form a complete orthonormal set

- Boundary condition of unit incident amplitude, such that $\sum_j \alpha^{(j)} C_0^{(j)} = 1$ or:

$$\boldsymbol{C}\alpha = \boldsymbol{u} \quad (3.6)$$

  where column vector $\boldsymbol{u}$ has first element = 1 and all other elements are 0

- From eq. 3.3: $$\alpha = \boldsymbol{C}^{-1}\boldsymbol{u} = \tilde{\boldsymbol{C}}^{*}\boldsymbol{u} \quad (3.7)$$

  and: $$\alpha^{(j)} = C_0^{*(j)} \quad (3.8)$$

Bloch wave analysis: multiple beams

- For centrosymmetric crystals:
  - $\boldsymbol{A}$ is real and symmetric
  - all eigenvalues and eigenvectors are real
  - $\boldsymbol{C}$ is real and orthogonal ($\tilde{\boldsymbol{C}} = \boldsymbol{C}^{-1}$)
  - n eigenvalues give a dispersion surface with n branches:

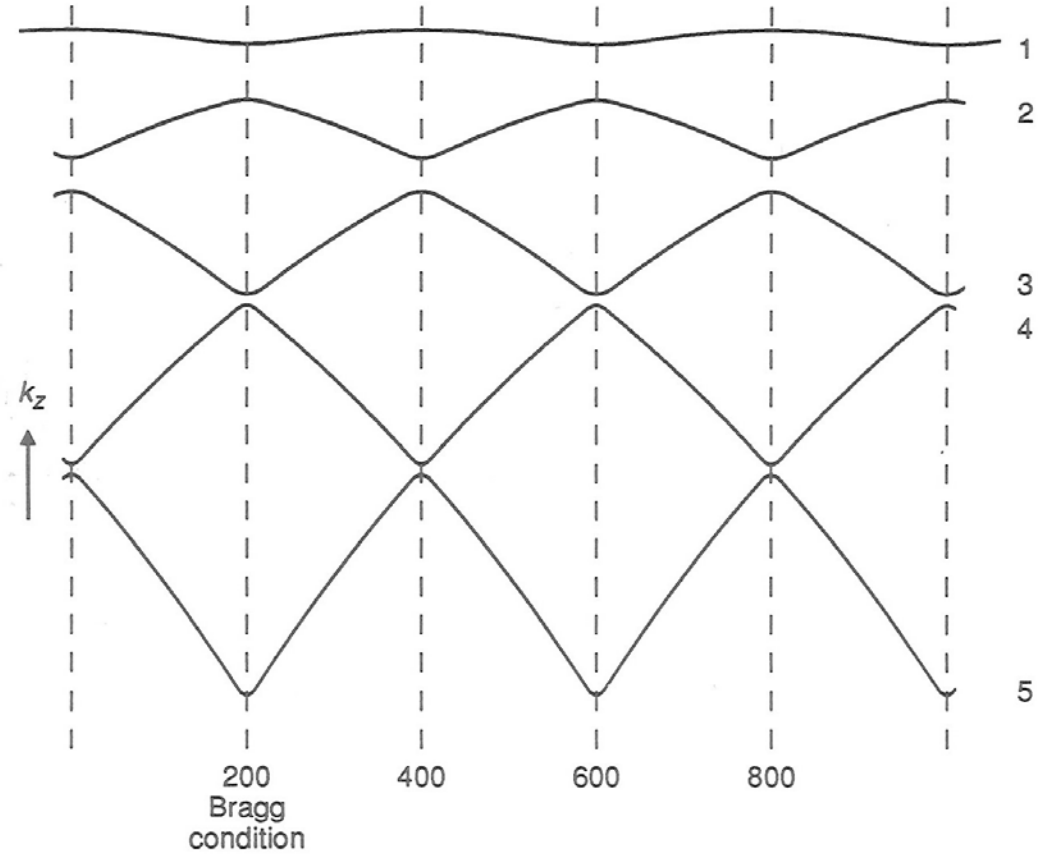

Schematic dispersion surface for systematic row of n reflections for Cu. From Humphreys and Bithell.

Bloch wave analysis: multiple beams

- General case, amplitude of diffracted beam leaving bottom surface of crystal given as (eq. 2.24):

$$\varphi_g(t) = \sum_j \alpha^{(j)} \sum_g C_g^{(j)} \exp\left(2\pi i k_z^{(j)} t\right)$$

- Write amplitudes of all diffracted beams as column vector $\boldsymbol{\varphi}$ where:

$$\boldsymbol{\varphi}(t) = \begin{pmatrix} \varphi_0(t) \\ \varphi_g(t) \\ \varphi_h(t) \\ \cdots \end{pmatrix} \tag{3.9}$$

- From 2.24 and 3.7:

$$\begin{aligned} \boldsymbol{\varphi}(t) &= \boldsymbol{C}\left[\exp\left(2\pi i k_z^{(j)} t\right)\right]_{\mathrm{D}} \boldsymbol{\alpha} \\ &= \boldsymbol{C}\left[\exp\left(2\pi i k_z^{(j)} t\right)\right]_{\mathrm{D}} \boldsymbol{C}^{-1}\boldsymbol{u} \end{aligned} \tag{3.10}$$

- These Bloch wave matrices can be solved by computational methods (e.g. Kirkland book)

Convergent beam electron diffraction

- Map beam intensities in function of $\vec{g}$ and s

Convergent beam electron diffraction

- 2-beam illustration with fully-focused beam (from J.-P. Morniroli)

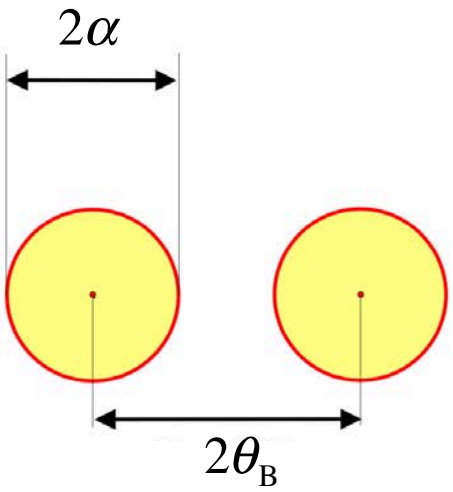

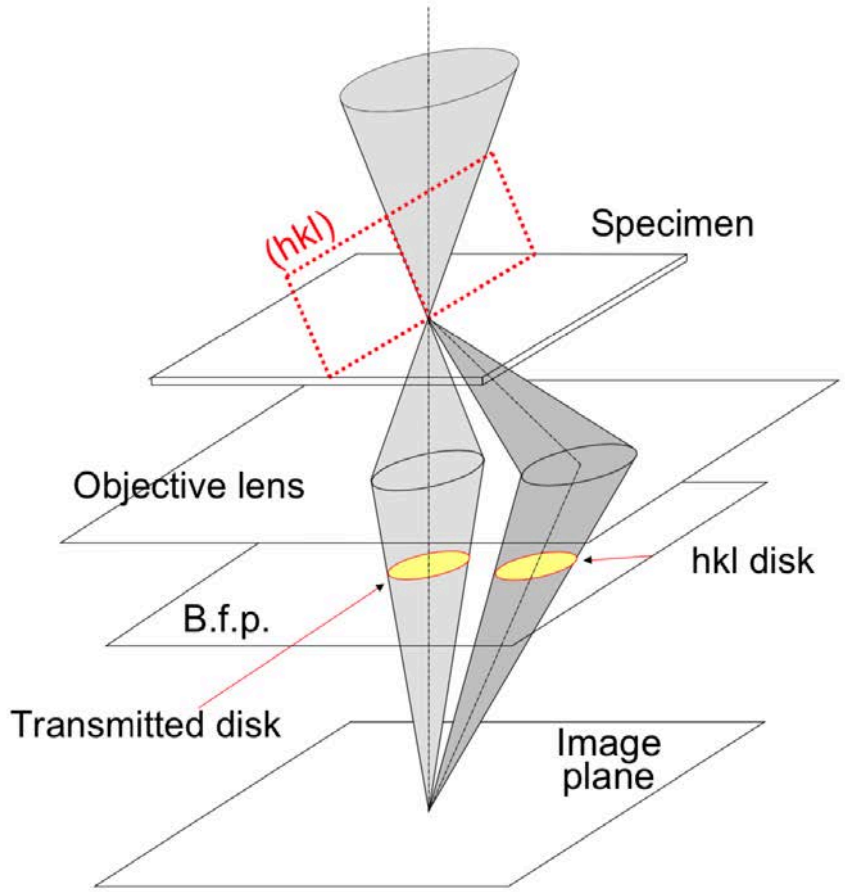

Convergent beam electron diffraction

- Diffracted beam CBED disc contains different ray paths that have sampled different excitation errors s
- Illustrate with Ewald sphere construction (diagram from J.-P. Morniroli)

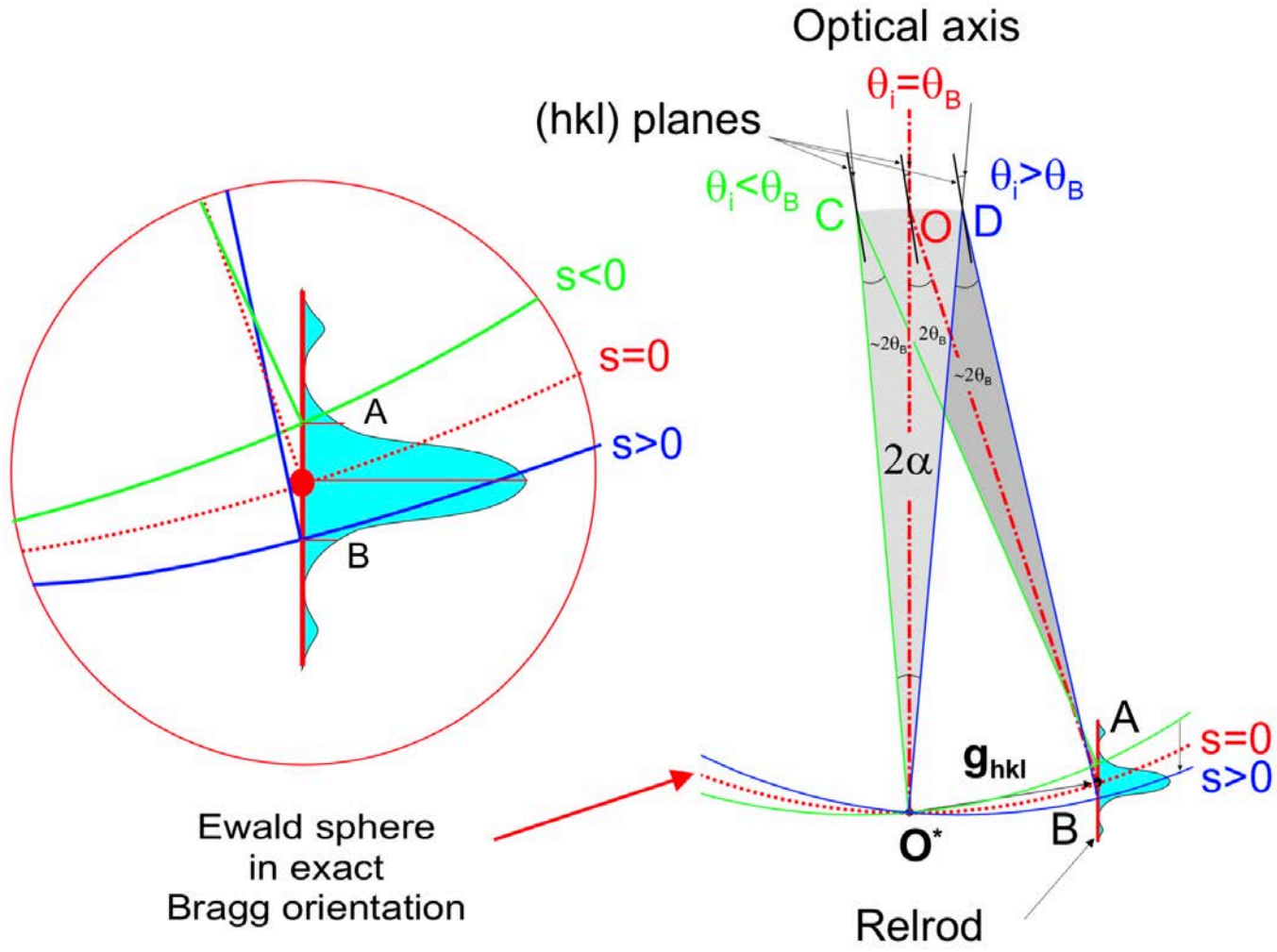

Bloch wave modelling and CBED

- Convergent beam electron diffraction (CBED) pattern simulations are probably the most common application of Bloch wave modelling, e.g. using JEMS
- In 2-beam condition, incident parallel rays at different angles lead to sampling of different excitation errors in diffracted beam disc:

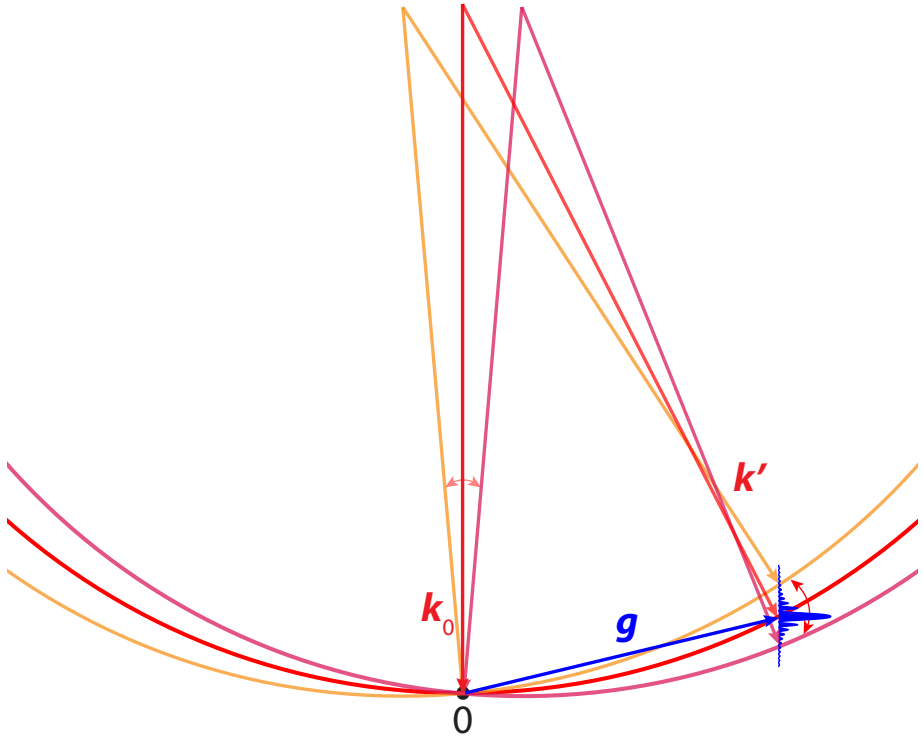

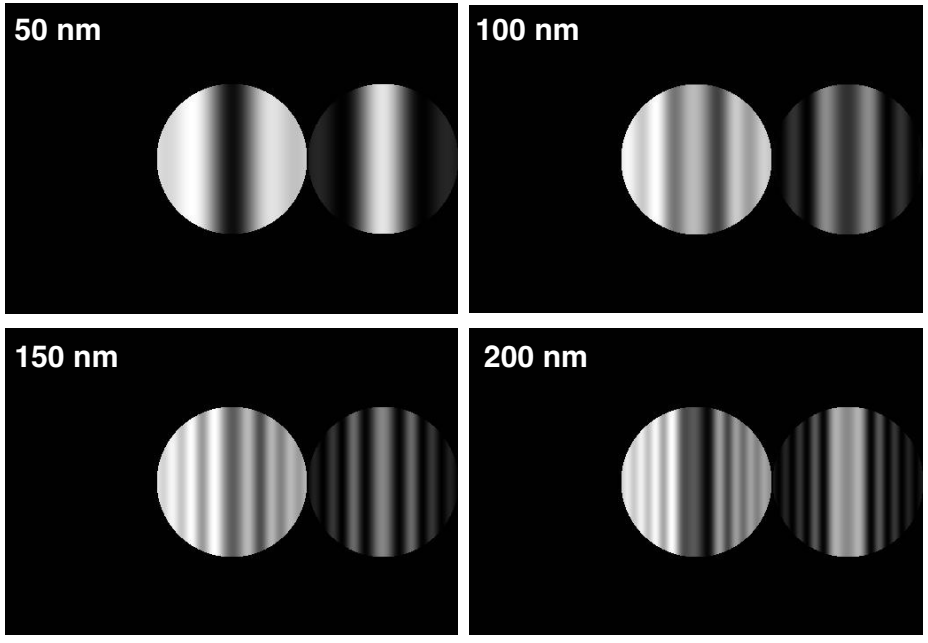

Simulations for Al with $\vec{g}_{002}$ excited for indicated t

Bloch wave modelling and CBED

- On zone axis, CBED patterns have complex patterns of fringes from the dynamical scattering, which can also be accurately simulated using Bloch wave modelling
- Case of Si on [0 0 1] zone axis:

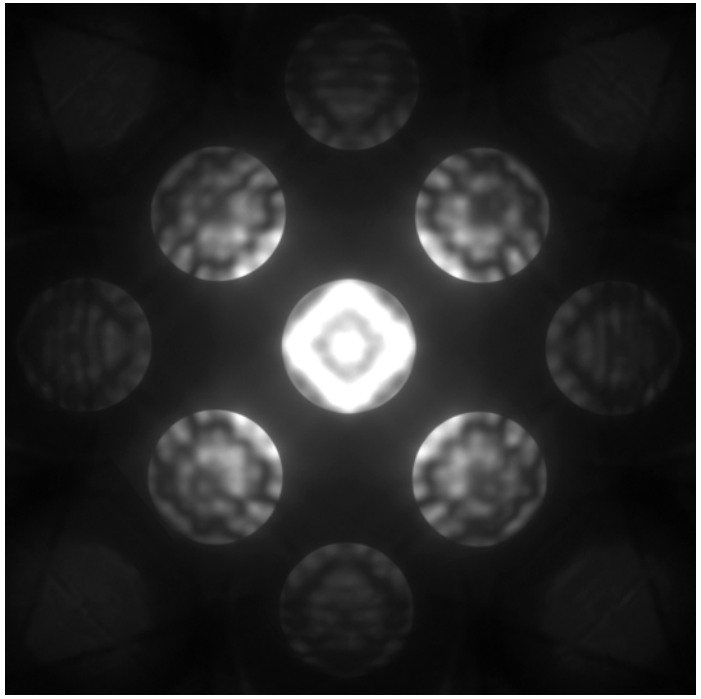

Experiment

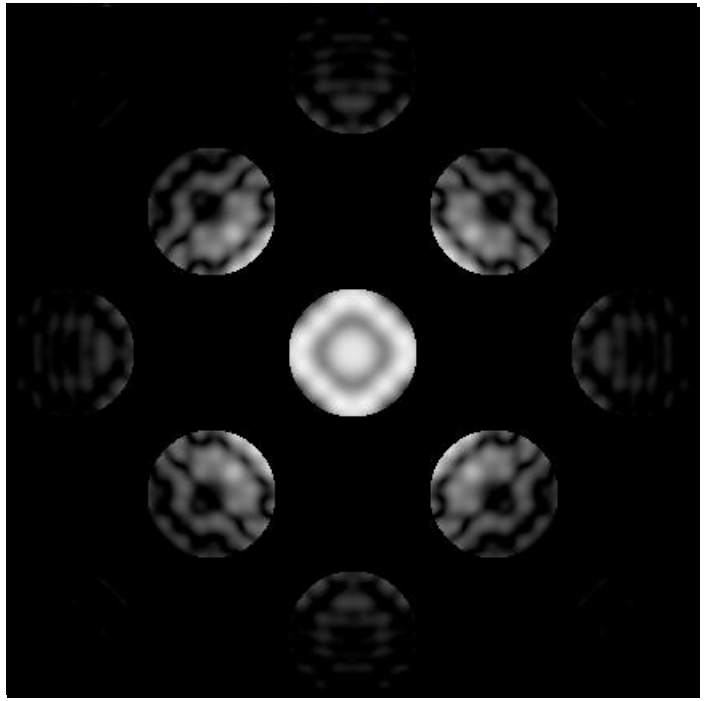

Simulation: 200 kV; t = 126nm;
4.1 mrad convergence semi-angle

CBED and polarity

- The difference in Bloch wave propagation down different atomic columns can be exploited to measure crystal polarity from CBED patterns
- Common use: identifying polarity in wurtzite crystal structure (P63mc) – GaN, ZnO, …

GaN atomic structure along [1 -1 0 0]:

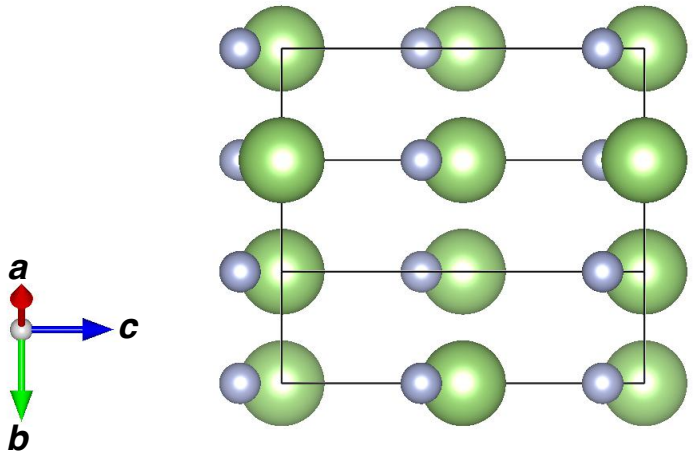

JEMS simulation: GaN [1 -1 0 0] ZA

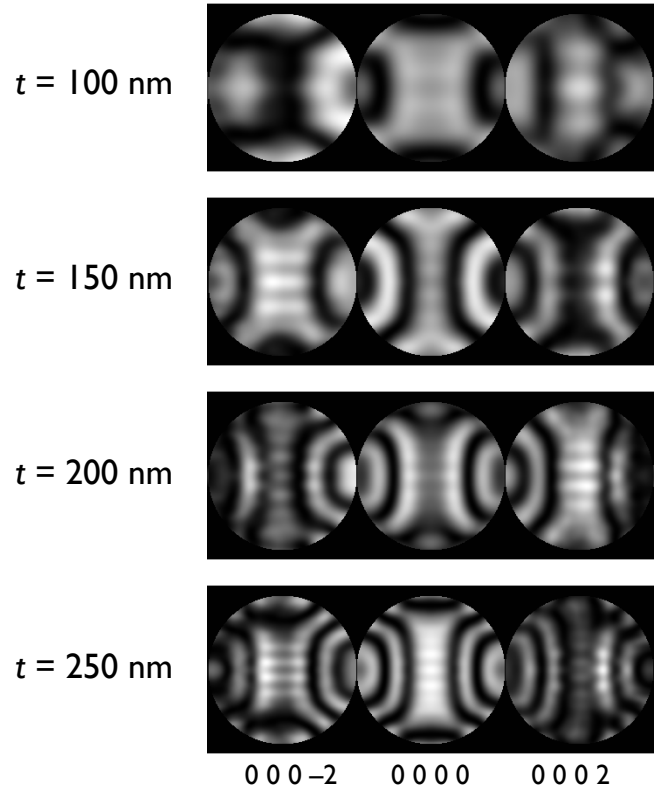

Electron channeling

- Already seen the relation of Bloch wave electron density to atomic columns for the 2-beam condition with $n = 2$ Bloch waves
- "Channeling" of Bloch waves down atomic columns even more significant in high resolution imaging of crystals on low index zone axes
- Applies to both plane wave (HRTEM) and focused probe (scanning TEM) illumination
- Schematic illustration:

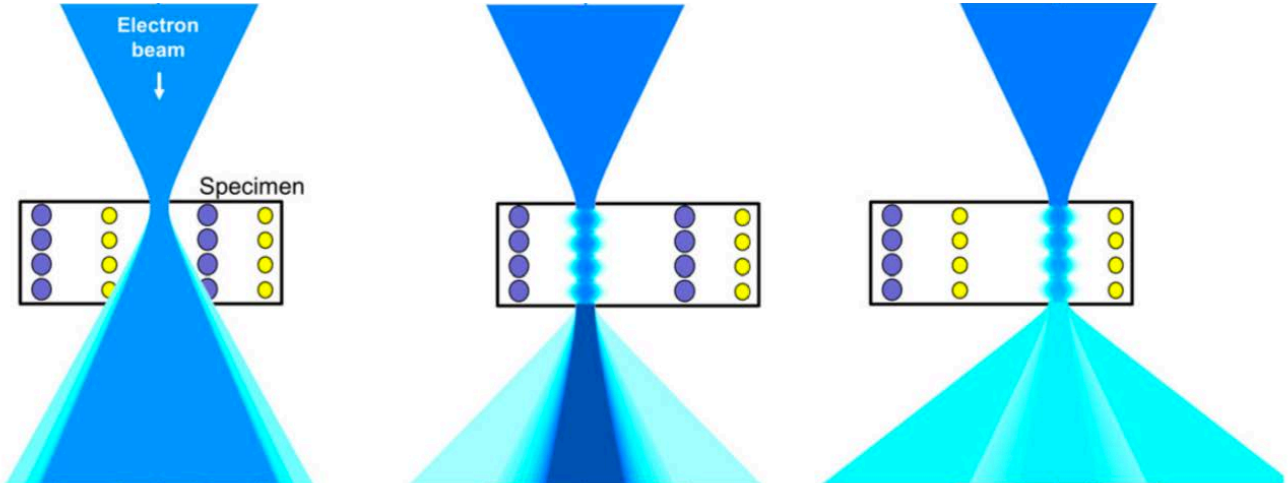

From: Findlay et al. Microscopy (2017) 3–14

1*s*-state Bloch wave

- Zone axis condition: wave function of propagating e^- beam can be expressed in form of Bloch wave eigenstates with the potential being formed by the 2D projection of the atomic column
- Catalogued by analogy to atomic orbitals (1*s*, 2*p*, 2*s*, …)

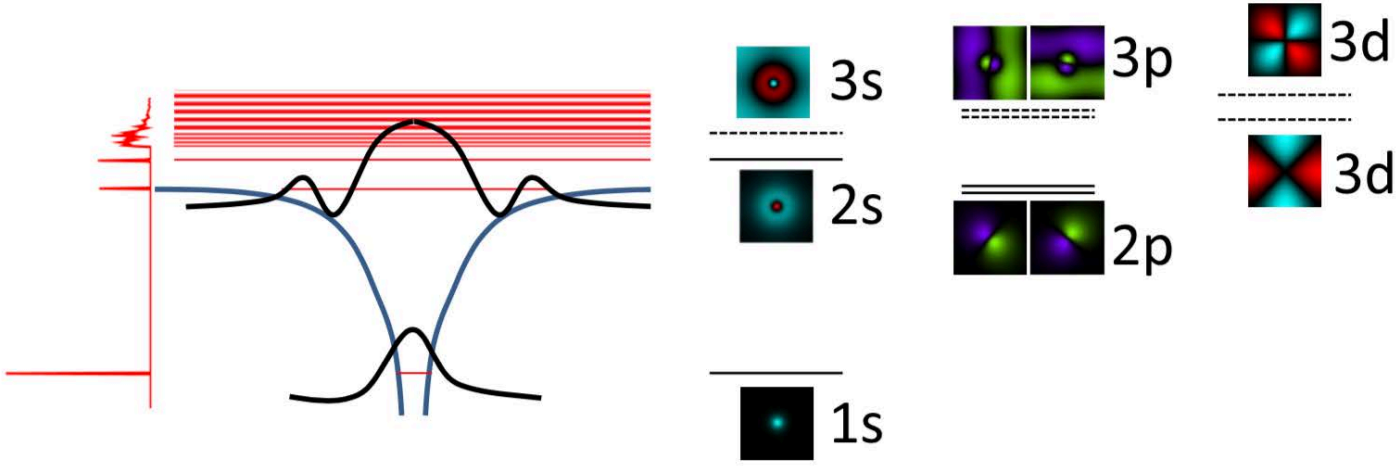

From: Wouters et al.
PRB **100** (2019) 184106

- Significance formalised into "1*s*-state approximation"

s-state Bloch wave model

- Assume atomic columns parallel to beam and well-separated
- Van Dyck and Op de Beeck introduced a specifically-conceived Bloch wave approach
- Adapted for HRTEM by Geuens and Van Dyck

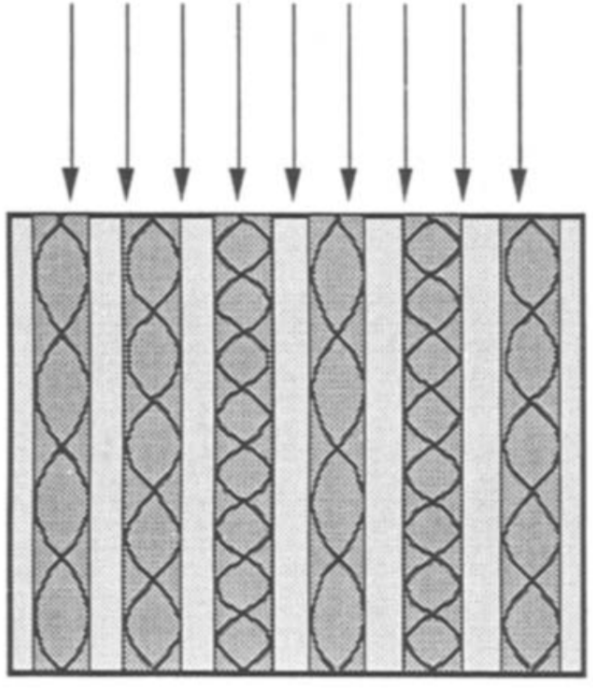

- Precept: wave function at exit surface mainly depends on projected structure
- Atomic column acts as guide or channel for electrons that can scatter dynamically without leaving column

Van Dyck and Op de Beeck Ultramicroscopy **64** (1996) 99–107
Geuens and Van Dyck Ultramicroscopy **93** (2002) 179–198

s-state Bloch wave model

- For propagation along z-axis can consider z-axis as time axis:

$$t = mz/hk \tag{3.11}$$

- Recall Schrödinger eq. 1.8, now use coordinate $\vec{\boldsymbol{r}}_\perp$ in the plane perpendicular to z:

$$\hat{H}\Psi\left(\vec{\boldsymbol{r}}_\perp,t\right) = i\hbar\frac{\partial\Psi\left(\vec{\boldsymbol{r}}_\perp,t\right)}{\partial t} \tag{3.12}$$

where:

$$\hat{H} = \frac{\hat{p}^2}{2m} + V\left(\vec{\boldsymbol{r}}_\perp,t\right) = -\frac{\hbar^2}{2m}\nabla^2_{\vec{\boldsymbol{r}}_\perp} - e\phi\left(\vec{\boldsymbol{r}}_\perp,t\right) \tag{3.13}$$

- Then obtain:

$$\frac{\partial}{\partial z}\Psi\left(\vec{\boldsymbol{r}}_\perp,t\right) = \frac{i}{4\pi k}\left[\nabla^2_{\vec{\boldsymbol{r}}_\perp} + V\left(\vec{\boldsymbol{r}}_\perp,z\right)\right]\Psi\left(\vec{\boldsymbol{r}}_\perp,t\right) \tag{3.14}$$

where:

$$V\left(\vec{\boldsymbol{r}}_\perp,z\right) = \frac{2me}{\hbar^2}\phi\left(\vec{\boldsymbol{r}}_\perp,z\right) \tag{3.15}$$

s-state Bloch wave model

- After considering only non-overlapping 1*s*-type bound states which are very localised to atomic cores, obtain:

$$\Psi\left(\vec{r}_\perp, z\right) = 1 + \sum_j C_j \Phi_j\left(\vec{r}_\perp - \vec{r}_\perp^{(j)}\right)\left[\exp\left(-i\pi \frac{E_j}{eE_0} kz\right) - 1\right] \qquad (3.16)$$

where each column has one eigenfunction Φ_j

- Therefore each column acts as a channel in which wave function oscillates periodically with depth. Periodicity proportional to atomic number Z

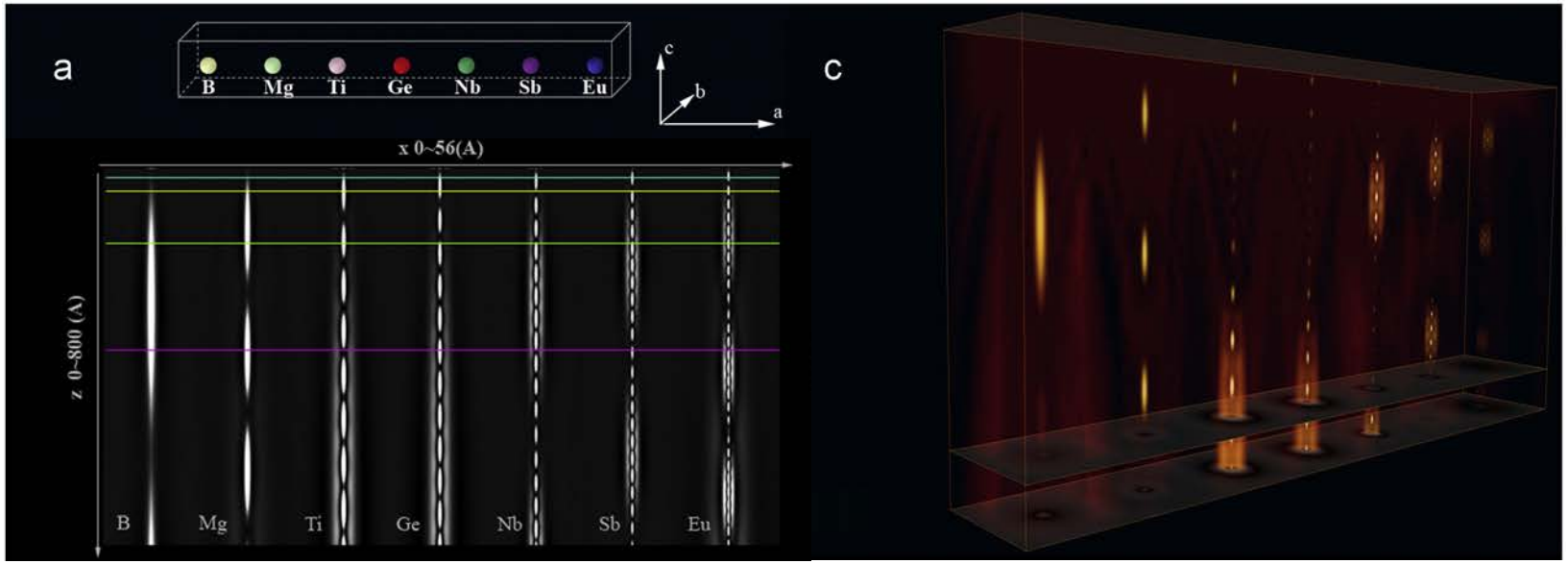

From: Xu et al. Ultramicrosc. **110** (2010) 535–542

1*s*-state and STEM imaging

- For atomic resolution STEM with a (sub-)Å convergent probe, the 1*s* state is the most relevant, having electron density amplitude strongly peaked on centre of atomic column
- At first approximation, high angle annular dark-field (HAADF) and annular bright field (ABF) images are consequence of the scattering of this 1*s*-state to their respective detectors

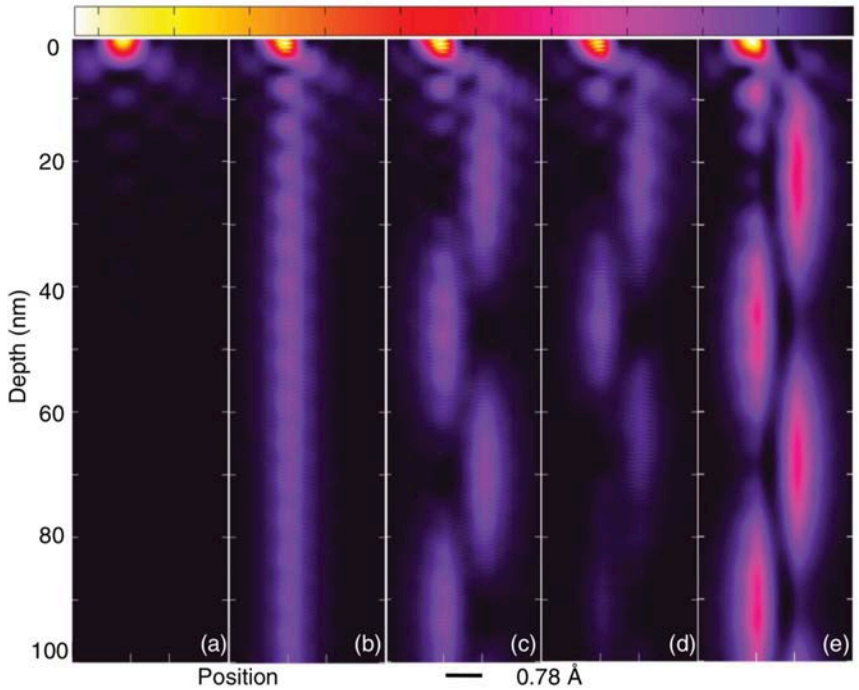

From: Hovden et al. PRB **86** (2012) 195415

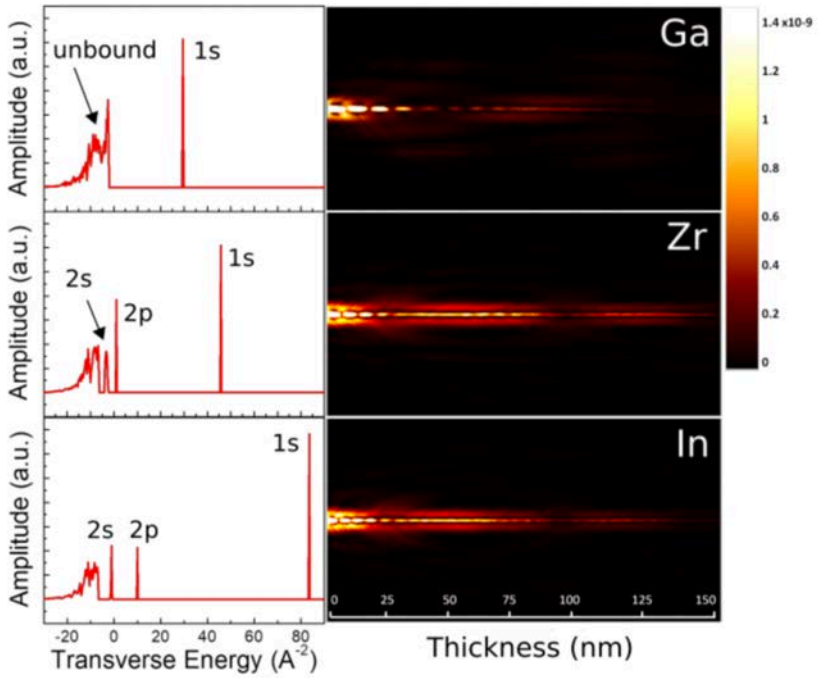

From: Wouters et al. PRB **100** (2019) 184106

Phonon scattering

Debye-Waller factor

- Modification of structure factor term to account for observed decrease in scattering efficiency from thermal vibrations of atoms
- F_g^T is temperature-dependent structure factor related to F_g and Debye-Waller M factor by:

$$F_g^T = F_g \exp(-M) \tag{3.17}$$

$$M = 8\pi^2 \left\langle (u)^2 \right\rangle \left(\frac{g}{2}\right)^2 = B\left(\frac{g}{2}\right)^2 \tag{3.18}$$

where $\left\langle (u)^2 \right\rangle$ is the mean-square displacement of the atom

- B is the temperature factor, values given in *International Tables for X-ray Crystallography*
- Because of g^2 term important for higher order reflections, e.g. for Au: $F_{555}^{RT} \approx 0.5 F_{555}$
- Concomitant effect on ξ_g

Diffuse scattering in diffraction

- Observe diffuse intensity between the sharp diffracted beams of selected area DPs
- When this intensity forms diffuse lines: termed “Kikuchi lines”

Si on [0 0 1] ZA

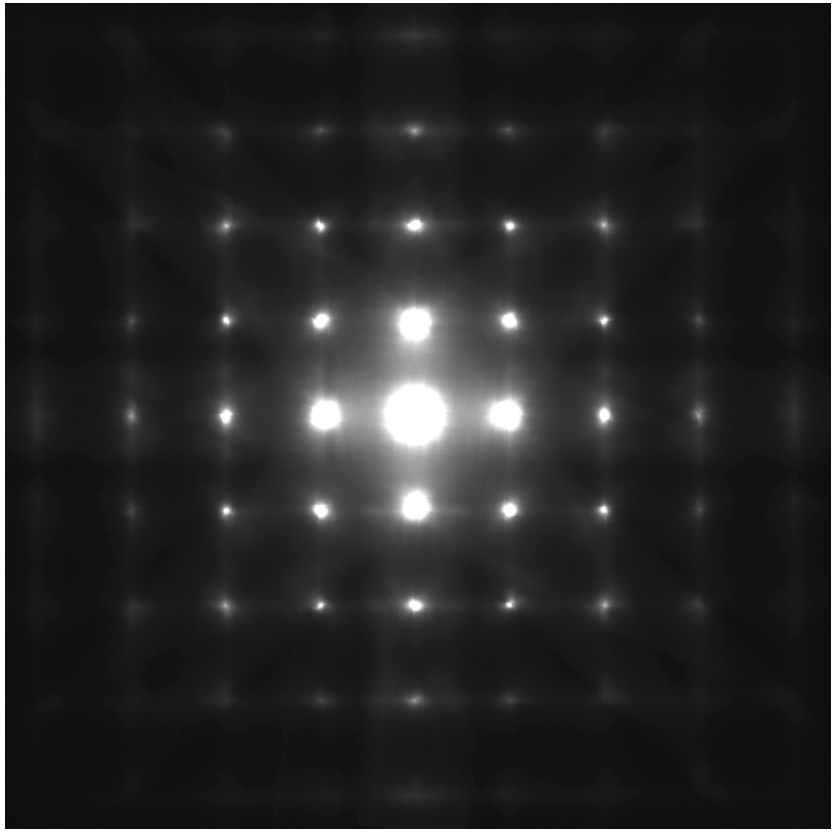

Si near a 2-beam condition

HAADF STEM imaging

- Integrate intensity from electrons scattered to high angles, beyond Bragg-diffracted beams
- Imaging is incoherent in nature, e.g. camera-like properties of contrast and focus

$LaVO_3$ thin film on $SrTiO_3$

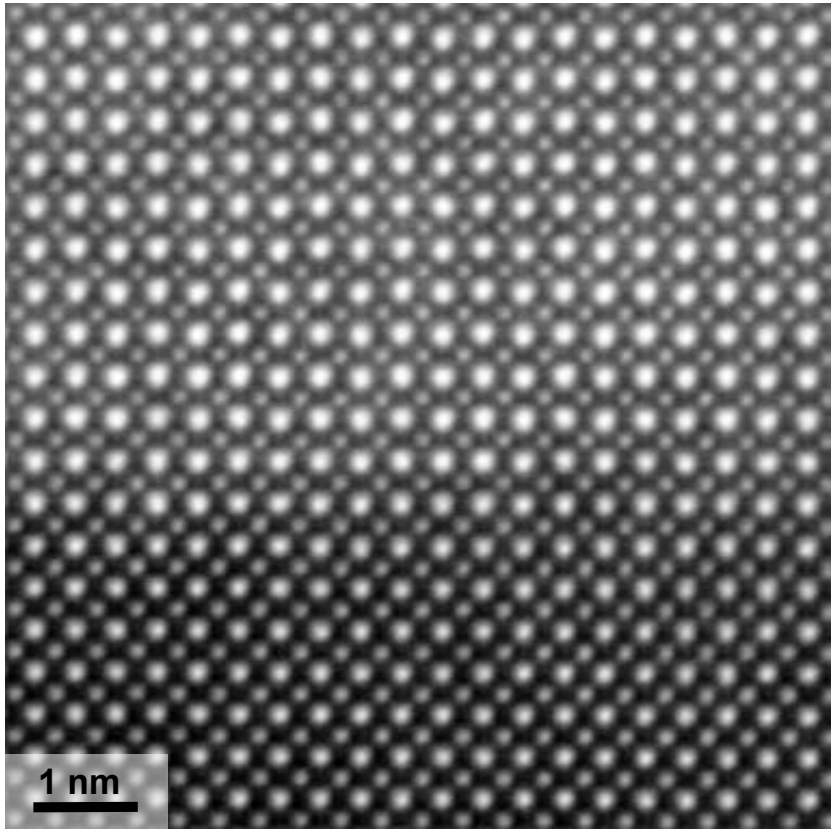

Edge of GaAs nanowire

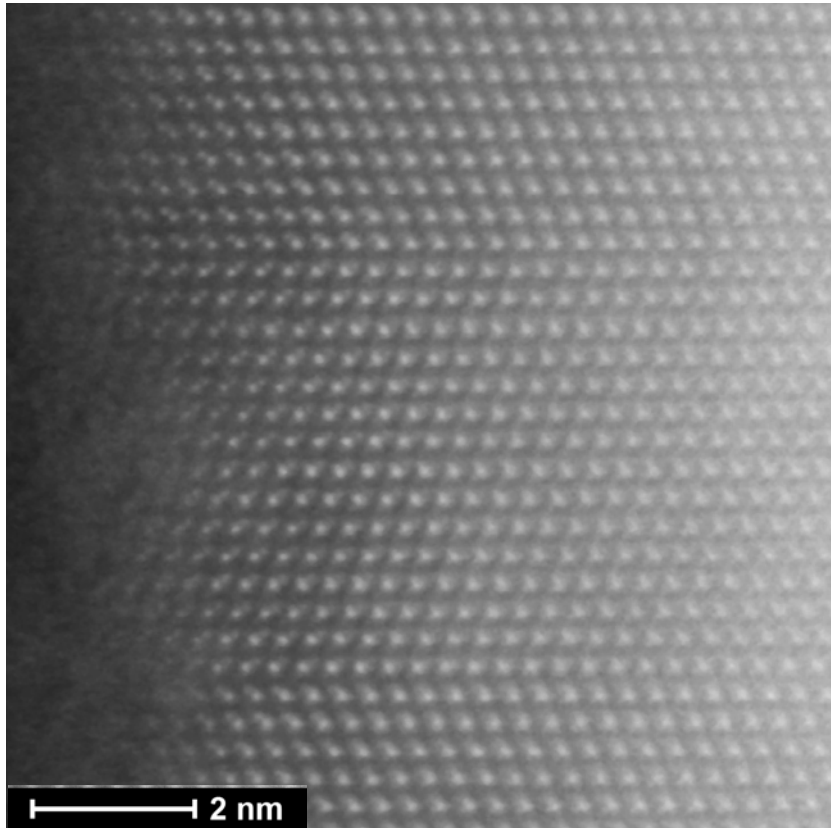

Absorption of 2-beam intensity

- Plot integrated line profiles of $I_0(t)$ and $I_g(t)$ of cleaved Si wedge at Bragg condition →
- Significant damping of intensities i.e. "absorption"
- Not accounted in model with: $I_g(t) = \sin^2(\pi t/\xi_g)$

$$I_0(t) = 1 - I_g(t)$$

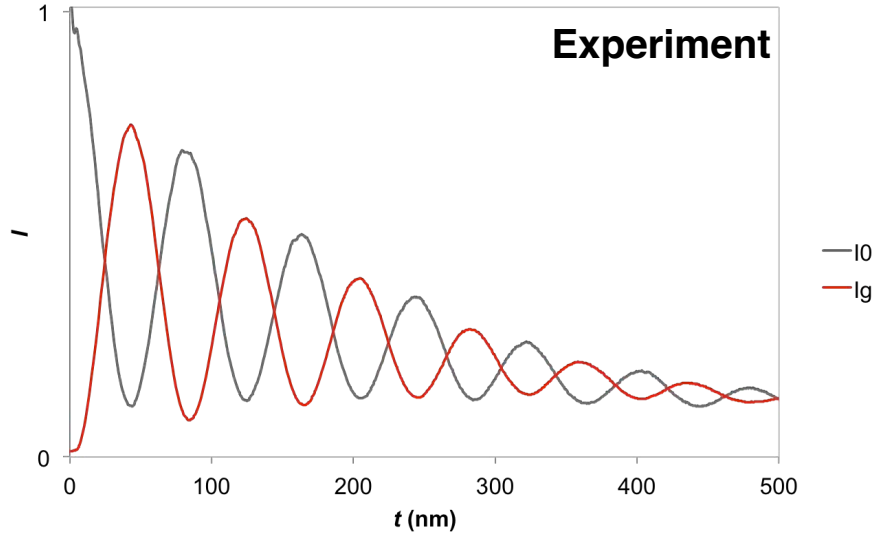

Bright-field

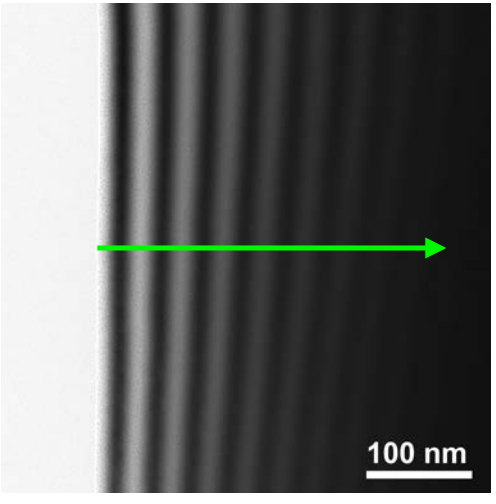

Dark-field

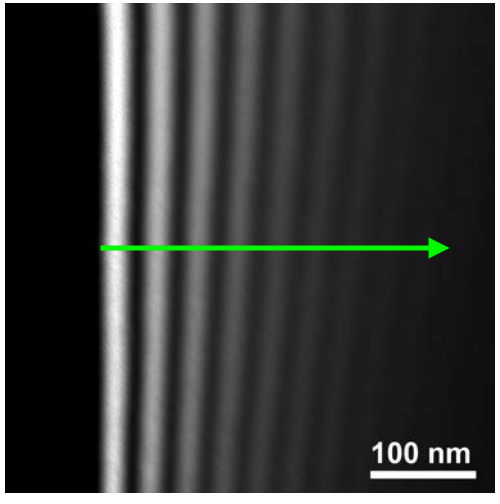

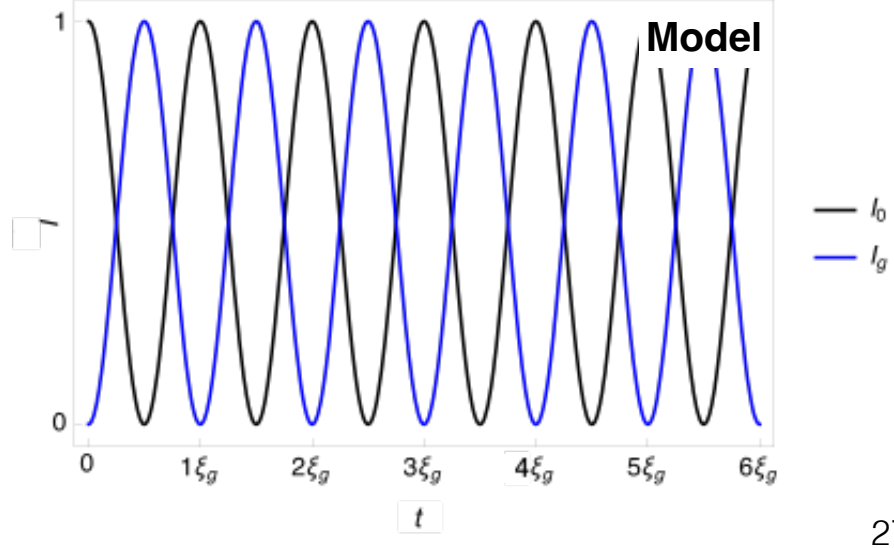

“Thermal diffuse scattering”

- Diffuse intensity between diffracted beams originally ascribed to “*thermal diffuse scattering*” (TDS)
- This is conceived as incoherent scattering caused by thermal vibrations in the crystal lattice – i.e. phonons
- The small, random displacements of atoms/atomic nuclei caused by these vibrations are considered to scatter the electron beam/wave function incoherently
- The Deybe-Waller factor and TDS are two sides of the same coin: the loss of coherent elastic scattering intensity is from its redistribution into incoherent diffuse intensity
- As a first approximation, the HAADF STEM image is formed from incoherent TDS of the highly localised 1*s*-state Bloch wave to the high angle annular detector
- Correlated to “absorption” of Bragg-diffracted beams, from depletion of Bloch waves as their electron density is incoherently scattered by phonon excitations

Single scattering cross-sections

- For single scattering, Amali and Rez derived the scattering cross-section for TDS as:

$$I(q) = \frac{d\sigma}{d\Omega} = \frac{\gamma^2}{4\pi^4 a_0^2} \frac{\left[Z - f_x(\vec{\mathbf{q}})\right]^2}{q^4} \left[1 - \exp\left(-\frac{Mq^2}{2\pi^2}\right)\right] \qquad (3.18)$$

- Plot of scattering cross-sections vs scattering angle (log scale for σ)
  - Short dashed line: Rutherford cross-section
  - Solid line: Mott scattering
  - Long dashed line: thermal diffuse scattering
- Indication of importance of TDS for HAADF STEM

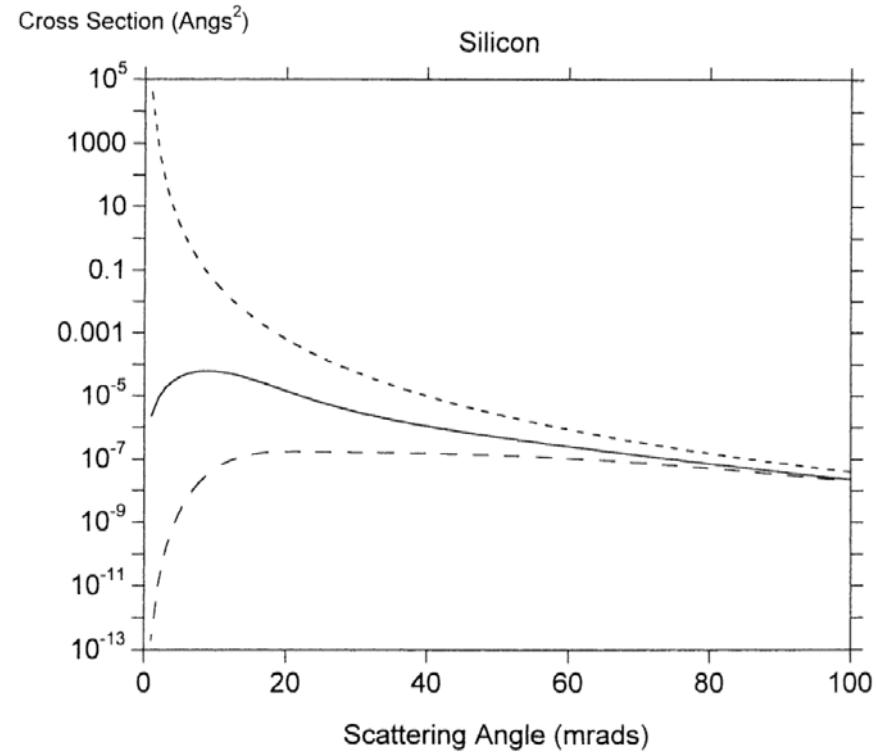

From: Rez Microsc. Microanal. **7** (2001) 356–362

Bloch wave model with “absorption”

- Incoherent scattering removes intensity from diffracted beams: termed “absorption” or depletion
- Can treat phenomenologically by incorporating imaginary potential into equations 2.14–3.10:

$$\begin{aligned} \phi(\vec{\boldsymbol{r}}) &\rightarrow \phi(\vec{\boldsymbol{r}}) + i\phi'(\vec{\boldsymbol{r}}) \\ V_g &\rightarrow V_g + iV_g' \\ U_g &\rightarrow U_g + iU_g' \end{aligned} \tag{3.19}$$

- The wave vectors also become complex: $\vec{\boldsymbol{k}}^{(j)} \rightarrow \vec{\boldsymbol{k}}^{(j)} - i\vec{\boldsymbol{u}}^{(j)}$ (3.20)

$\Longrightarrow$ each Bloch wave physically attenuated as it propagates through the crystal

Bloch wave model with “absorption”

- Equation 2.33 becomes:

$$\Psi(\vec{\boldsymbol{r}}) = \sum_j \alpha^{(j)} \sum_g C_g^{(j)} \exp\left[2\pi i\left(\vec{\boldsymbol{k}}^{(j)} + \vec{\boldsymbol{g}}\right)\cdot \vec{\boldsymbol{r}}\right] \exp\left(-2\pi \vec{\boldsymbol{u}}^{(j)} \cdot \vec{r}\right) \tag{3.21}$$

- $\alpha^{(j)}$ replaced by exponentially attenuated amplitude $\alpha^{(j)}(z)$:

$$\alpha^{(j)}(z) = \alpha^{(j)} \exp\left(-2\pi u^{(j)} z\right) \tag{3.22}$$

- Setting equations 3.19 in equations 3.1 and 3.2 gives a complex general matrix that can be solved by diagonalization using computer programs.

2-beam Bloch waves with “absorption”

- At exact Bragg condition, for 2-beam approximation can be shown:

$$u^{(1)} = \frac{1}{2\kappa_z}\left(U_0' + U_g'\right) \qquad (3.23)$$

$$u^{(2)} = \frac{1}{2\kappa_z}\left(U_0' - U_g'\right) \qquad (3.24)$$

- Mean absorption length:

$$\xi_0' = \kappa_z / U_0' \qquad (3.25)$$

- Anomalous absorption length:

$$\xi_g' = \kappa_z / U_g' \qquad (3.26)$$

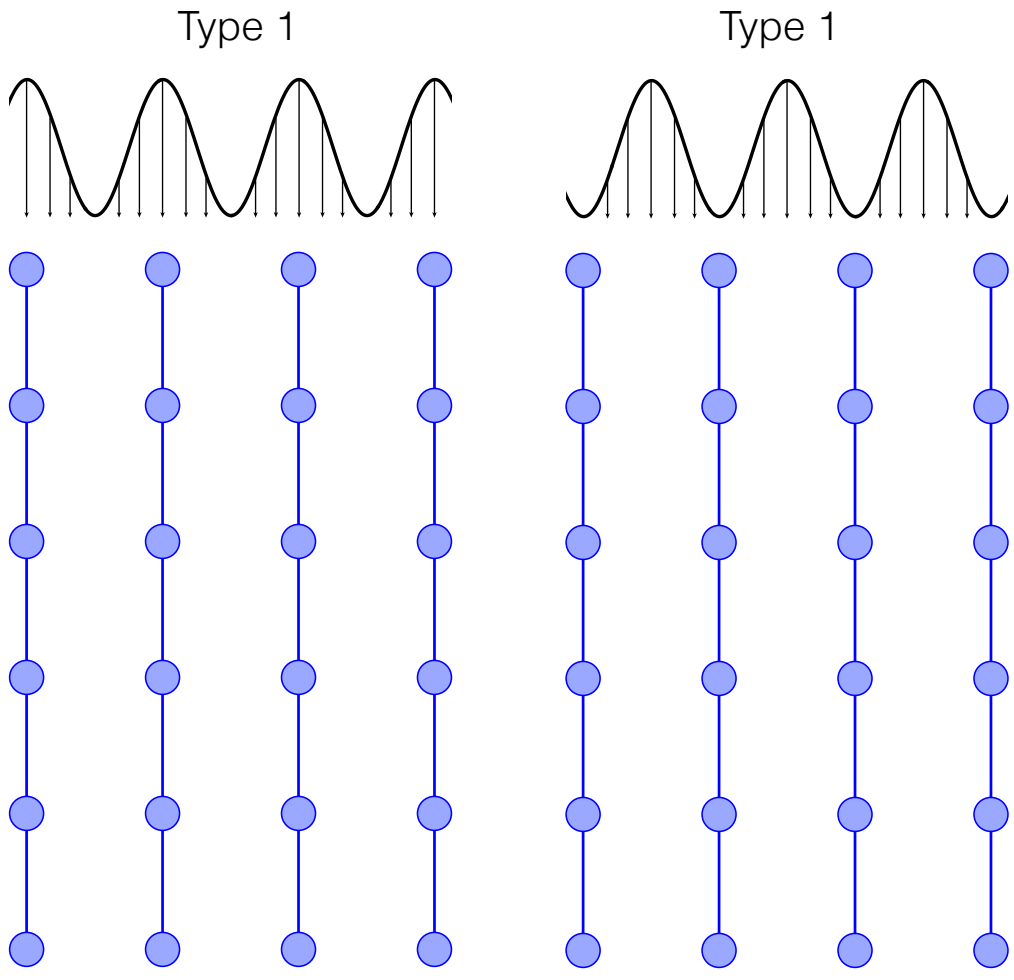

2-beam Bloch waves with “absorption”

- Include ξ_0' and ξ_g' in modelling of thickness fringes at the exact Bragg condition
- Use “common” values of: $\xi_0' = 10\xi_g \quad \xi_g' = 15\xi_g$
- Experimental data and model fit very well!

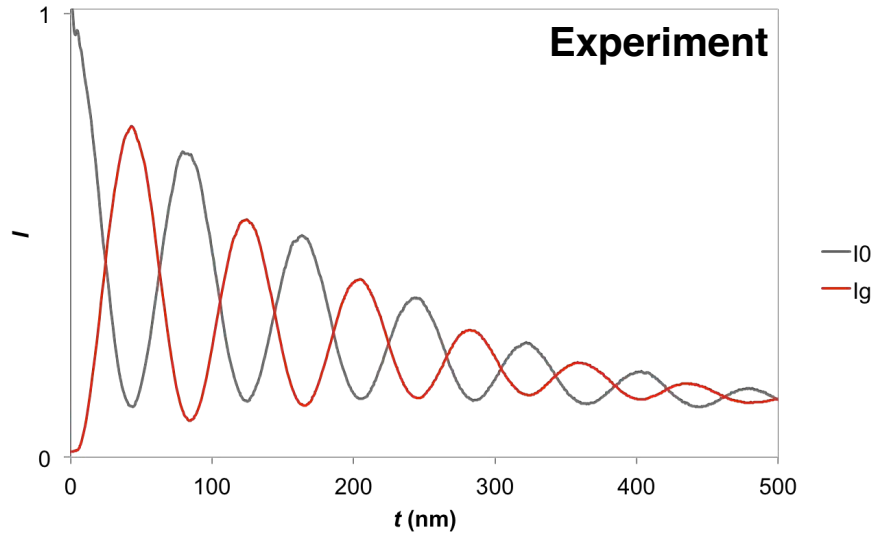

Bright-field

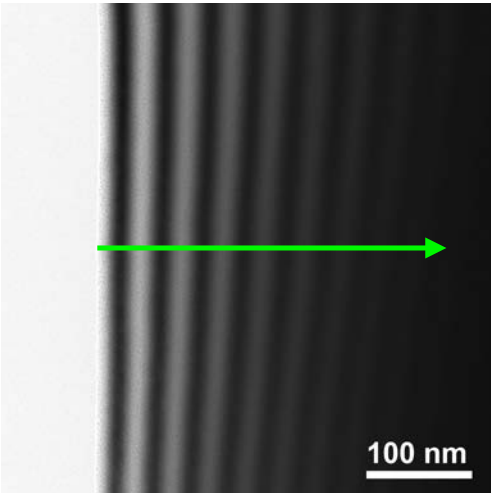

Dark-field

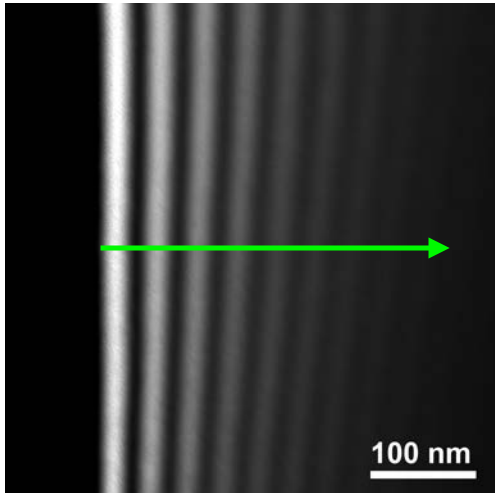

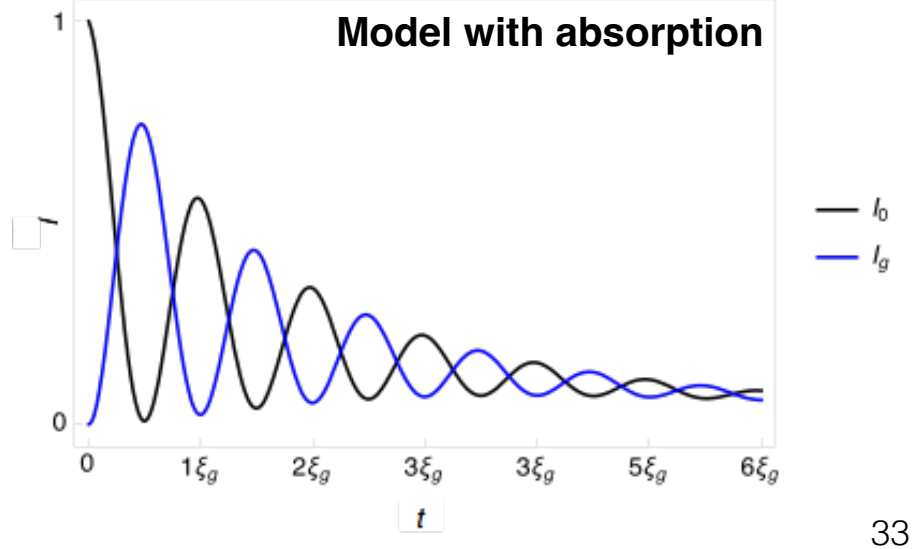

Frozen phonon model

- The phenomenological absorption approach is insufficient for:
  - simulating the diffuse contribution of phonon scattering to diffraction patterns
  - simulating HAADF STEM images where intensity primarily from incoherent phonon scattering of the 1*s*-state Bloch wave.
- To solve this problem, Loane and Silcox introduced the “frozen phonon model”: Acta Cryst. A**47** (1991) 267–278.
- Models elastic scattering from atoms displaced from their equilibrium positions by thermal vibrations.
- Popular and relatively efficient simulation method, which can give a very good match to experimental data, e.g.: QSTEM, Dr Probe, abTEM…

Frozen phonon model

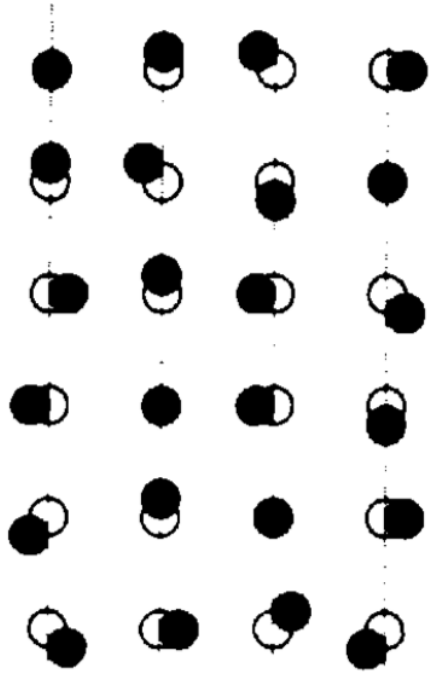

- Concept: fast electron traverses crystal much faster than oscillation period of the atom
- The “electron sees a snapshot of the atom frozen midvibration”.
- Each electron “sees” a different configuration. The contributions of different electrons are summed incoherently in the detector plane.
- In practice this is implemented by a Monte Carlo integration.
- The scattering is determined by propagating the incident wave function across the atomic configuration using a multi-slice method.
- Typically uses the Einstein model of independent simple harmonic oscillators to simulate the displaced atoms.
- *Fully elastic approach* – is this physically correct?

QM model of phonon excitation

- Les Allen et al. introduced quantum mechanically correct model of phonon scattering: Forbes et al. PRB **82** (2010) 104103
- Introduces the QM exchange of phonon excitation into the Schrödinger equation
- Schrödinger equation modified to:

$$\left[-\frac{\hbar^2}{2m}\nabla_{\vec{r}}^2 + H_c(\vec{\tau}) + H'(\vec{r},\vec{\tau})\right]\Psi(\vec{r},\vec{\tau}) = E(\vec{r},\vec{\tau}) \qquad (3.27)$$

H_c is the Hamiltonian for all the crystal particles

H' describes the interaction of the incident e⁻ with the crystal particles

E is total energy of system

$\vec{r}$ is coordinate of incident e⁻

$\vec{\tau} = \{\vec{r}_1,\ldots,\vec{r}_N\}$ is set of all position vectors referring to particles in the crystal

QM model of phonon excitation

- $\Psi(\vec{r},\vec{\tau})$ expanded in terms of eigenfunctions of the crystal Hamiltonian $H_c(\tau)$

$$\Psi(\vec{r},\vec{\tau}) = \sum_m \psi_m(\vec{r}) a_m(\vec{\tau}) \tag{3.28}$$

where the normalised wave function $a_m(\vec{\tau})$ represents the mth stationary state of the crystal (of energy ε_m) and satisfies the equation:

$$H_c(\vec{\tau}) a_m(\vec{\tau}) = \varepsilon_m a_m(\vec{\tau}) \tag{3.29}$$

$a_0(\vec{\tau})$: initial state of crystal (not necessarily ground state)

$\psi_0(\vec{r})$ in eq. 3.28: fast e⁻ after elastic scattering

$\psi_m(\vec{r})$ $(m \neq 0)$: describes the fast e⁻ after transition in which crystal is changed from $a_0(\vec{\tau})$ to $a_m(\vec{\tau})$

QM model of phonon excitation

- Energy of e⁻ in state $\psi_0(\vec{r})$ is given by:

$$E_0 = E - \varepsilon_0 \tag{3.30}$$

- For inelastic scattering, the energy associated with $\psi_m(\vec{r})$, i.e. after the inelastic scattering, is:

$$E_m = E - \varepsilon_m \tag{3.31}$$

- Therefore energy-loss of incident e⁻ after exciting crystal from initial to mth state is:

$$E_{loss} = E_0 - E_m = \varepsilon_m - \varepsilon_0 \tag{3.32}$$

QM model of phonon excitation

- Assume nuclear and electronic subsystems are decoupled, and that electronic subsystem is not excited, giving this factorisation:

$$a_m(\vec{\tau}) = b(\vec{\tau}_e)a_m(\vec{\tau}_n) \tag{3.33}$$

giving:

$$\Psi(\vec{\boldsymbol{r}},\vec{\tau}) = b(\vec{\tau}_e)\sum_m \psi_m(\vec{\boldsymbol{r}})a_m(\vec{\tau}_n) \tag{3.34}$$

- Then propose *ansatz* for the wave function of the system:

$$\Psi(\vec{\boldsymbol{r}},\vec{\tau}) = b(\vec{\tau}_e)a(\vec{\tau}_n)\varphi(\vec{\boldsymbol{r}},\vec{\tau}_n) \tag{3.35}$$

where $a(\vec{\tau}_n)$ is associated with the nuclear subsystem and $\varphi(\vec{\boldsymbol{r}},\vec{\tau}_n)$ with the fast e^-

QM model of phonon excitation

- Leads to equation:

$$-\frac{\hbar^2}{2m}\nabla^2_{\vec{r}}\varphi(\vec{r},\vec{\tau}_n)+\tilde{H}'(\vec{r},\vec{\tau}_n)\varphi(\vec{r},\vec{\tau}_n)=E_0\varphi(\vec{r},\vec{\tau}_n) \tag{3.36}$$

where:

$$\tilde{H}'(\vec{r},\vec{\tau}_n)=\int b^*(\vec{\tau}_e)H'(\vec{r},\vec{\tau})b(\vec{\tau}_e)\mathrm{d}\vec{\tau}_e \tag{3.37}$$

- Equation 3.36 can be solved using the multislice method for a set of nuclear coordinates $\vec{\tau}_n$

- Following this, the probability distribution of fast e⁻ modelled by the quantum mechanical average over nuclear coordinates is derived as:

$$I(\vec{r})=I(\vec{r}_\perp,z)=\int\left|\varphi(\vec{r}_\perp,z,\vec{\tau}_n)\right|^2\left|a_0(\vec{\tau}_n)\right|^2\mathrm{d}\vec{\tau}_n \tag{3.38}$$

- Integral can be solved via a Monte Carlo calculation, where $\left|a_0(\vec{\tau}_n)\right|^2$ acts as a probability distribution and $\varphi(\vec{r}_\perp,z,\vec{\tau}_n)$ are obtained via the multislice method

QM model of phonon excitation

- Need to consider many electrons, where electrons incident at different times during a measurement scatter from different initial crystal states, from a thermal statistical ensemble

- Measurement then modelled as incoherent sum of e⁻ scattered from different initial states:

$$I(\vec{\boldsymbol{r}}_\perp, z) = \sum_j I_j(\vec{\boldsymbol{r}}_\perp, z) = \int \left|\varphi(\vec{\boldsymbol{r}}_\perp, z, \vec{\tau}_n)\right|^2 \left\{\sum_j \left|a_i(\vec{\tau}_n)\right|^2\right\} \mathrm{d}\vec{\tau}_n$$

$$= \int \left|\varphi(\vec{\boldsymbol{r}}_\perp, z, \vec{\tau}_n)\right|^2 P(\vec{\tau}_n) \mathrm{d}\vec{\tau}_n \qquad (3.39)$$

- If crystal modelled as set of independent harmonic oscillators, jth atom has probability distribution:

$$P\left(\vec{\tau}_n^{(j)}\right) = \sqrt{\frac{1}{2\pi\left\langle\left(u^{(j)}\right)^2\right\rangle}} \exp\left[\frac{\left(\tau_n^{(j)} - \vec{\boldsymbol{R}}^{(j)}\right)^2}{\left\langle\left(u^{(j)}\right)^2\right\rangle}\right] \qquad (3.38)$$

where: $\vec{\boldsymbol{R}}^{(j)}$ is the equilibrium position of the atom;

$\left\langle\left(u^{(j)}\right)^2\right\rangle$ is the mean-squared displacement of the atom (see Debye-Waller slide)

QM model of phonon excitation

- With this model elastic and inelastic phonon scattered contributions can be separated
- Applied to simulating plane wave illumination diffraction pattern of 20 nm thick $SrTiO_3$
  - (a): full intensity; (b) elastically-scattered e^- only; (c) inelastically-scattered e^-

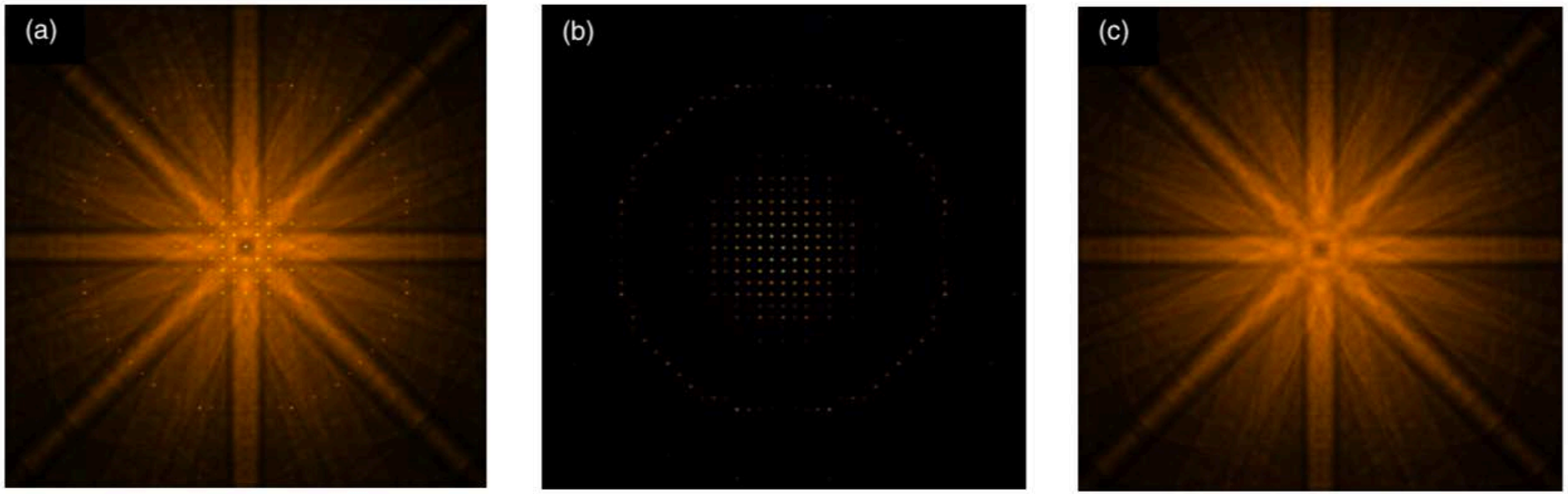

QM model of phonon excitation

- With this model elastic and inelastic phonon scattered contributions can be separated
- Applied to simulating CBED pattern of 6 nm thick $SrTiO_3$
  - (a): full intensity; (b) elastically-scattered e^- only; (c) inelastically-scattered e^-

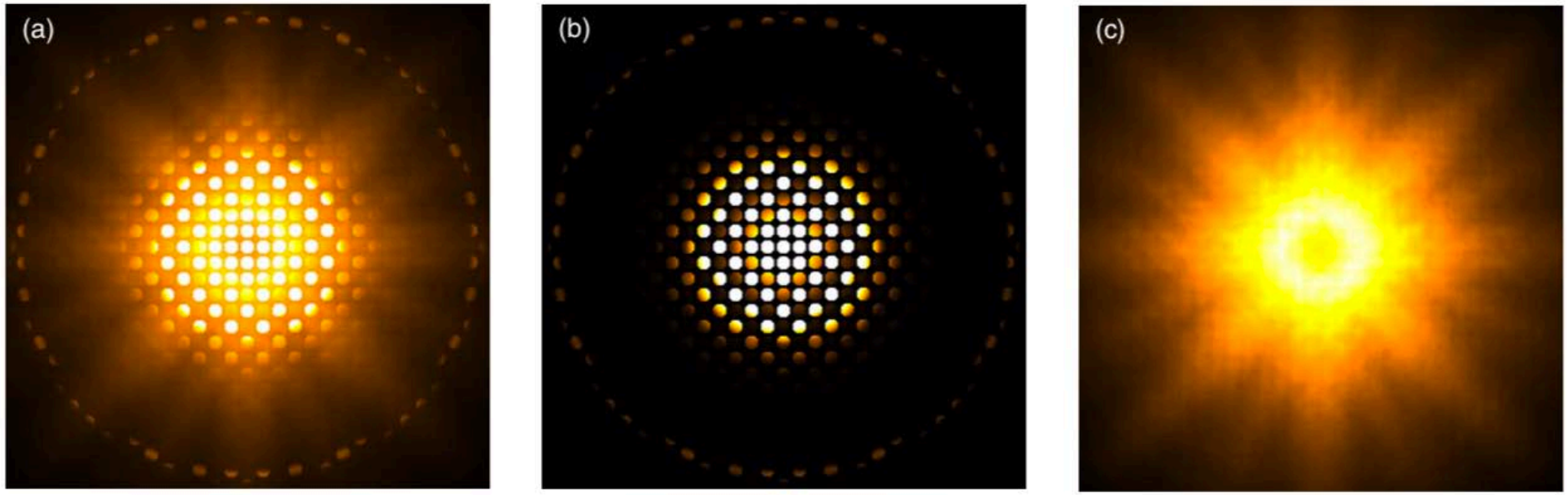

- Used to understand anomalous HAADF contrast in: https://arxiv.org/abs/2401.08798

QM model of phonon excitation

- Term-by-term analysis shows that the frozen phonon and QM models are actually equivalent for the end result.
- However, the fully elastic approach of the frozen phonon is physically incorrect. This has now been proven using ultra-low-loss electron energy-loss spectroscopy! TDS corresponds to a phonon excitation with ΔE.
- The QM model that correctly represents the inelastic nature of phonon scattering is available for use in the μSTEM simulation software, which can simulate diffraction patterns, HRTEM and STEM images, EDXS, EELS…

PACBED HAADF STEM

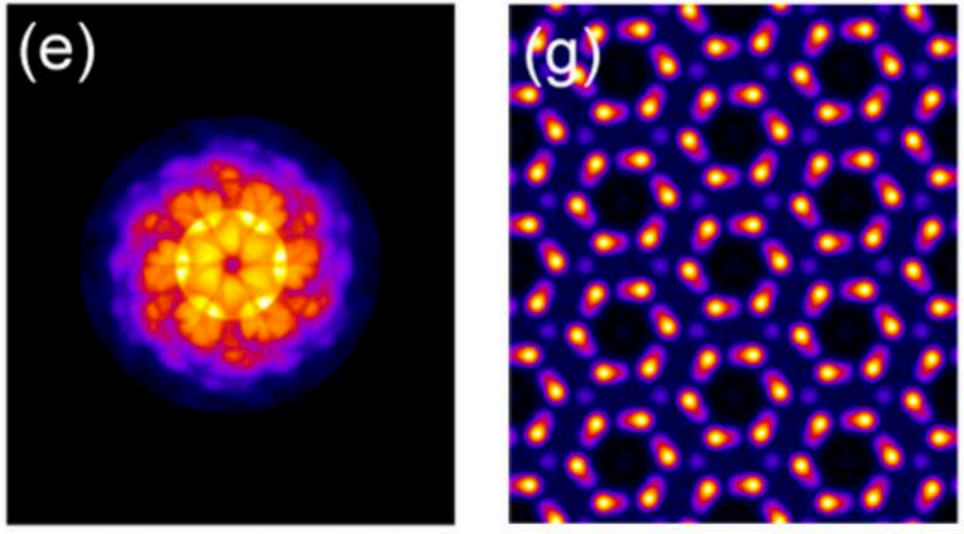

Les J. Allen et al. Ultramicroscopy **151** (2015) 11–22

- V6 including plasmon scattering: https://github.com/ju-bar?tab=repositories

Bibliography

- Earl J. Kirkland, “Advanced Computing in Electron Microscopy”, Springer. https://link.springer.com/book/10.1007/978-1-4419-6533-2
- A. Amali and P. Rez, “Theory of Lattice Resolution in High-angle Annular Dark-field images” – derivation of single-scattering cross section for TDS using Bose-Einstein model
- S. J. Pennycook and D. E. Jesson, “High-Resolution Incoherent Imaging of Crystals” – Bloch wave analysis showing 1*s*-state dependence of HAADF contrast
- D. Van Dyck and M. Op de Beeck, “A simple intuitive theory for electron diffraction” – 1*s*-state model
- R. F. Loane et al., “Thermal Vibrations in Convergent-Beam Electron Diffraction” – Introduction of the frozen phonon model
- B. D. Forbes et al., “Quantum mechanical model for phonon excitation in electron diffraction and imaging using a Born-Oppenheimer approximation” and L.J. Allen et al. “Modelling the inelastic scattering of fast electrons” – QM model used in μSTEM